International Journal of Latest Trends in Engineering and Technology
Vol.(9)Issue(4), pp.221-228
DOI: http://dx.doi.org/10.21172/1.94.33
e-ISSN:2278-621X

EXPERIMENTAL ANALYSIS OF IMPROVING MRR ON µEDM UNDER THE INFLUENCE OF ELECTROMAGNETIC FIELD

Aman Kumar[1], P. S. Satsangi[2]

Abstract-This paper presents a study of the influential effect of machining parameters like type of material, voltage, feed rate, and spindle speed on machining characteristics like MRR (material removal rate) in magnetic field assisted µEDM-drilling process. Two workpieces titanium alloy (Ti-6Al-4V) and AISI D2-Steel has been studied simultaneously under same orthogonal array to better understand the effect of electromagnetic field (EMF) on magnetic and non-magnetic materials. Wedge shaped electromagnets has been used to produce pulsed magnetic field and continuous magnetic field. The workpiece materials used were 1 mm thick while the tool was a 400 µm diameter tungsten carbide electrode. L_{18} Orthogonal array was used for carrying out experiment where one factor is taken at two levels and other factors are taken at three levels. Taguchi Methodology is used to establish a relationship between type of material, voltage, feed rate, magnetic field and spindle speed on output characteristics MRR. Furthermore, the optimal settings of process parameters in terms of mean response characteristic are established by analyzing response curves and the ANOVA Tables. In the last stage of work, estimation of optimum performance characteristics is validated by performing confirmation experiments. The proposed models could be realized as significant tools for mass production using magnetic field.

Keywords: µEDM, MRR, L_{18} Orthogonal array, pulsed magnetic field.

1. INTRODUCTION

µEDM is capable process in the field of miniaturization. The unique capability of µEDM process is it can also be associated with different processes for producing the minuscule parts (Yu, Masuzawa and Fujino, 1998; Takahata and Gianchandani, 2002; Prakash et al., 2017). The µEDM is a process which uses thermo-electric energy to erode the material from a conductive workpiece and a conductive electrode in presence of a good dielectric fluid (Kumar and Satsangi, 2014). In this process, both the electrodes are aligned together for some selected gap voltage. Electrode material erodes due to spark generation (Alting et al., 2003). There are two categories of µEDM: die-sinking and wire-cut. Die-sinking reproduces shape of the tool is used whereas in wire-cut µEDM, a metal wire is used for cutting a work-piece. In recent years, tremendous developments in µEDM have emphasized on the mass production of micro-designs.

Wansheng et al (2002) performed µEDM on Ti-alloy and reported slow condensation results in long sized debris. Opposite effect is also reported on use of steel plates, so it's easier to machine steel. Yan and Lai (2007) machined Ti-alloy with WEDM and reported about thermal oxidation due to high heat. Due to this machining of Ti-alloy is difficult. Kuriakose and Shunmugam (2004) also reported formation of oxides with WEDM and hence burning effect on cutting surface is seen. Bhattacharya, Batish and Bhatt, (2015) studied a hybrid EDM process on various die steels. In case of D2 steel, they used tungsten powder along with magnetic field and found WC powder improved micro-hardness by 2 times and magnetic field quickens the MRR. Siva, Parivallal and Kumar, (2014) studied machining of d2 steel on µEDM. They concluded that MRR is directly proportional to current. Overcut and taper does go incremental with increment in voltage. Jafferson et al. (2014) compared magnetic assistance with hybrid vibro-magneto assistance and found that µEDM-milling of titanium with 230G permanent magnets resulted in improved MRR and reduced TWR while with hybrid system, MRR reduced and TWR increased. Chu et al. (2015) applied 0.3T magnets on µEDM. They reported improvement in MRR due to less machining time and better debris removal.

Although many researches has been carried out using many difficult-to-machine materials as a centre of the study. Still many scopes have been found to enhance the MRR and to make micro EDM process industry viable. In the present work, an effort is reported regarding enhancement in production of micro-parts. Magnetic field assisted µEDM-drilling process is used to study the effect of input parameters on MRR. Electromagnets are used to produce pulsed magnetic field (0-0.4T) and continuous magnetic field of 0.4 T. All the experiments are performed on highly accurate DT-110 µEDM. Taguchi methodology is used to investigate the effect of magnetic field on performance measures of µEDM. An effort is also made to compare the magnetic and non-magnetic materials at the same platform i.e. under the influence of induced magnetic field; hence two materials titanium alloy (Ti-6Al-4V) and AISI D2-Steel are also taken as one of the input variable.

---

[1] PhD Research Scholar, Mechanical Engineering Department, Punjab Engineering College (Deemed to be University), Chandigarh

[2] Professor, Mechanical Engineering Department, Punjab Engineering College (Deemed to be University), Chandigarh

2. EXPERIMENTAL SET UP

A highly accurate DT-110 μEDM (available in Punjab Engineering College, Chandigarh) is used for performing the experimental work. It works on RC-type pulse generator and has 6 capacitance setting values, along with variable voltage (80V – 130V). Both capacitance and voltage are responsible for producing the discharge energy. A solid cylindrical special tool made of tungsten carbide with 400 micron diameter is used. The drilling operation was performed on rectangular shaped (1mm thick) workpieces. The workpieces are made of titanium alloy (Ti-6Al-4V) and AISI D2-Steel. Both materials are investigated under influence of no electromagnetic field (NEMF), pulsed electromagnetic field (PEMF) and continuous electromagnetic field (CEMF) using L18 array. The chemical-composition of workpiece materials along with magnetic nature is shown in Table 1 and Table 2 respectively.

Table 1 Chemical-Composition of AISI D2 Steel

Element	C	Si	Mn	Cr	Ni	Mo	V	Fe	Nature
(in Wt %)	1.49	0.30	0.207	11.64	0.228	0.794	1.0	Balanced	Magnetic

Table 2 Chemical-Composition of Titanium Alloy (Ti-6Al-4V)

Element	Al	V	C	Fe	Ti	Nature
(in wt %)	5.600	4.500	0.020	0.012	Balanced	Non-Magnetic

While performing the pilot experimentation, it is learnt that if same small diameter (0.4 mm diameter) tool are more and errors cannot be nullified the chances of wobbling of tool. This problem commonly occurs in electrodes with diameters ≤ 500 μm. To avoid this problem, specially designed non-fluted WC tool with large shank diameter (as shown in fig. 1) is used. The removal of debris is achieved by the side flushing of dielectric (EDMM oil). After preliminary investigations, the input parameters are selected as per table 3.

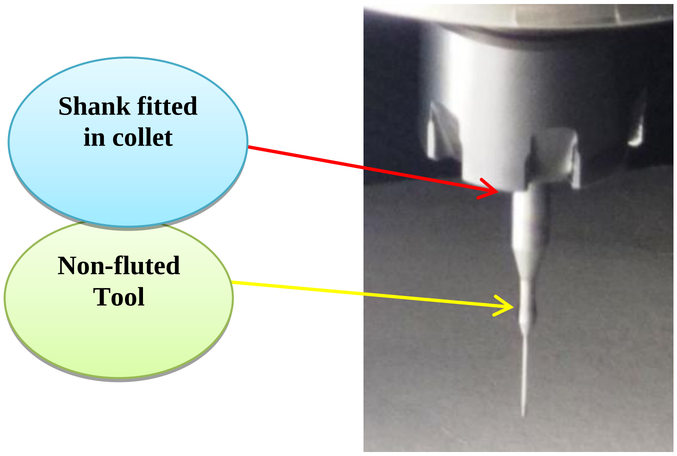

Fig. 1 Easy holding of Actual tool in collet (due to large shank diameter)

Table 3 input parameters selected for L_{18} orthogonal array

Inputs	Measurement	L(1)	L(2)	L(3)
Materials	-	Titanium	D2 Steel	-
Voltage	V	110	120	130
Feed Rate	μm/s	4	6	8
Magnetic field	Tesla	No Magnetic Field	Pulsed Magnetic Field	Continuous Magnetic Field
RPM of tool	Rev/Min.	250	500	750
Capacitance = 0.4 μF is taken as Constant				

Most of the researches have used the permanent magnet based magnetic field (Kumar and Satsangi, 2016); only a few has reported about importance of electromagnetic field at macro level machining (Chattopadhyay et al., 2008); and almost no research is available at μEDM level. An actual application of electromagnetic field setup is shown in fig. 2. The advantage of using electromagnets is these are fully controllable which is impossible in case of permanent magnets. The setup formed is not a simple electromagnetic field setup; it is capable of producing pulsed magnetic field and continuous magnetic field as per requirement of the user.

MRR (Material Removal Rate) in µEDM is the volumetric change per unit time. It is one of the substantial characteristic to measure and achieve. MRR is designated by mm^3/Minute. Basic equation of MRR is (Yan et al., 2002; Puertas, Luis and Álvarez, 2004; S and D, 2010):

$$\mathrm{MRR} = \frac{\text{Volume removed from work–material } (\mathrm{mm}^3)}{\text{Time of machining (in Minute)}} \qquad 1$$

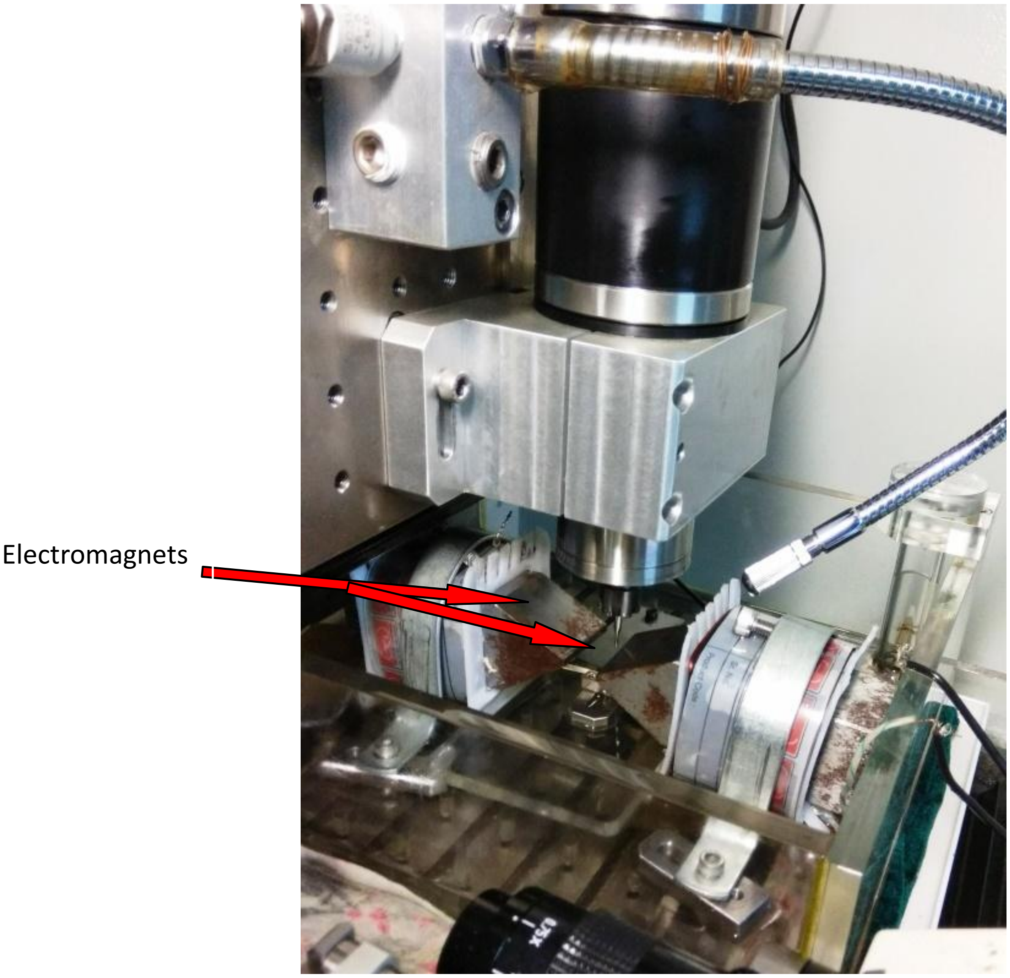

fig. 2 Actual setup of Electromagnets used

3. ANALYSIS BASED ON TAGUCHI METHOD FOR MRR

The experiments were planned by using the parametric approach of the Taguchi's L_{18} Orthogonal Array (OA). The response characteristics data are provided in Table 4. The analysis of the data is done by using the standard procedure. The average values and S/N ratio of the response characteristics for each parameter at different levels are calculated from experimental data. The main effects of process parameters for raw data and S/N data are plotted. Moreover, effect of each process parameter on output characteristics are examined by analyzing the response curves. The significant process parameters are identified by using analysis of variance (ANOVA). The ANOVA for raw data and S/N data is performed to analyze the effect of process parameters on performance measures. The optimal settings of process parameters in terms of mean response characteristic are established by analyzing response curves and the ANOVA Table.

Further, the effect of µEDM process parameters i.e. type of work-material, voltage, feed rate, electro-magnetic field and spindle speed on the selected output parameter (MRR) has been discussed. The type of work-material is varied at two levels, whereas voltage, feed rate, electro-magnetic field and spindle speed are varied at level one, two and three. Each experiment is replicated for three times to observe the exact effect of individual parameter on output response characteristic.

Table 4 Observed Values of MRR and S/N ratio

INPUT PARAMETERS						RESPONSES			
	A	B	C	D	E	RAW DATA			S/N Ratio
						MRR (mm3/min)			
Experiment No.	Materials	Voltage (V)	Feed Rate (µm/sec)	Electro-magnetic field	Spindle Speed (R.P.M.)	R1	R2	R3	
1	Ti-alloy	110V	4	No Magnetic Field	250	0.00524565	0.006004987	0.005370334	-45.17400487
2	Ti-alloy	110V	6	Pulsed Magnetic Field	500	0.005803903	0.006048044	0.005836028	-44.59319051
3	Ti-alloy	110V	8	Continuous Magnetic Field	750	0.005434926	0.00550109	0.005658546	-45.14681791
4	Ti-alloy	120V	4	No Magnetic Field	500	0.006398234	0.006342109	0.006211344	-43.99148399
5	Ti-alloy	120V	6	Pulsed Magnetic Field	750	0.007230005	0.0072012	0.006951927	-42.94506113
6	Ti-alloy	120V	8	Continuous Magnetic Field	250	0.006757014	0.007019422	0.006885719	-43.24206493
7	Ti-alloy	130V	4	Pulsed Magnetic Field	250	0.008586704	0.008272316	0.008141897	-41.58975923
8	Ti-alloy	130V	6	Continuous Magnetic Field	500	0.008141897	0.007858701	0.007893018	-41.98001303
9	Ti-alloy	130V	8	No Magnetic Field	750	0.006833653	0.006025004	0.006694449	-43.7581695
10	D2-steel	110V	4	Continuous Magnetic Field	750	0.00548495	0.005921216	0.005695139	-44.8945533
11	D2-steel	110V	6	No Magnetic Field	250	0.005033768	0.004946016	0.005358184	-45.84233066
12	D2-steel	110V	8	Pulsed Magnetic Field	500	0.005819302	0.00554865	0.005172251	-45.20223512
13	D2-steel	120V	4	Pulsed Magnetic Field	750	0.006693184	0.006464655	0.006922229	-43.49727725
14	D2-steel	120V	6	Continuous Magnetic Field	250	0.006136142	0.006490361	0.006272754	-44.02046069
15	D2-steel	120V	8	No Magnetic Field	500	0.005880025	0.005730533	0.005663341	-44.79781303
16	D2-steel	130V	4	Continuous Magnetic Field	500	0.007400594	0.007830306	0.007554133	-42.39650111

17	D2-steel	130V	6	No Magnetic Field	750	0.006026763	0.006102914	0.006620168	-44.10482751
18	D2-steel	130V	8	Pulsed Magnetic Field	250	0.007522918	0.008127438	0.007881152	-42.12261048

Effect on Work-material Removal Rate (MRR):

The raw data for average values of MRR and S/N ratio for each parameter was analyzed for type of work-material at two levels (L1 and L2) and voltage, feed rate, electro-magnetic field and spindle speed at three levels (L1, L2 and L3). The results so obtained are presented in Table 5 in form of raw data calculations for MRR at various levels. From the means table and observing fig. 3, Highest MRR is seen on Ti-alloy (L1) at settings gap-voltage 130 V (L3), feed rate 4µm/s (L1), pulsed electro-magnetic field (L2) and low spindle speed 250 R.P.M. (L1) i.e. $A_1B_3C_1D_2E_1$.

Table 5 Main Effects of MRR (Raw Data) at various levels

Level	Type of Materials	Voltage (V)	Feed Rate (µm/sec)	Electro-magnetic field	Spindle Speed (R.P.M.)
L1	**0.00668**	0.005549	**0.006697**	0.005916	**0.00667**
L2	0.006307	0.006514	0.006442	**0.006901**	0.006507
L3		**0.007417**	0.006342	0.006663	0.006303
DELTA	0.000372	0.001868	0.000355	0.000985	0.000366
Rank	3	1	5	2	4
L1, L2 and L3 represent level of parameters 1, 2 and 3, where DELTA is the main effect of the corresponding parameter.					

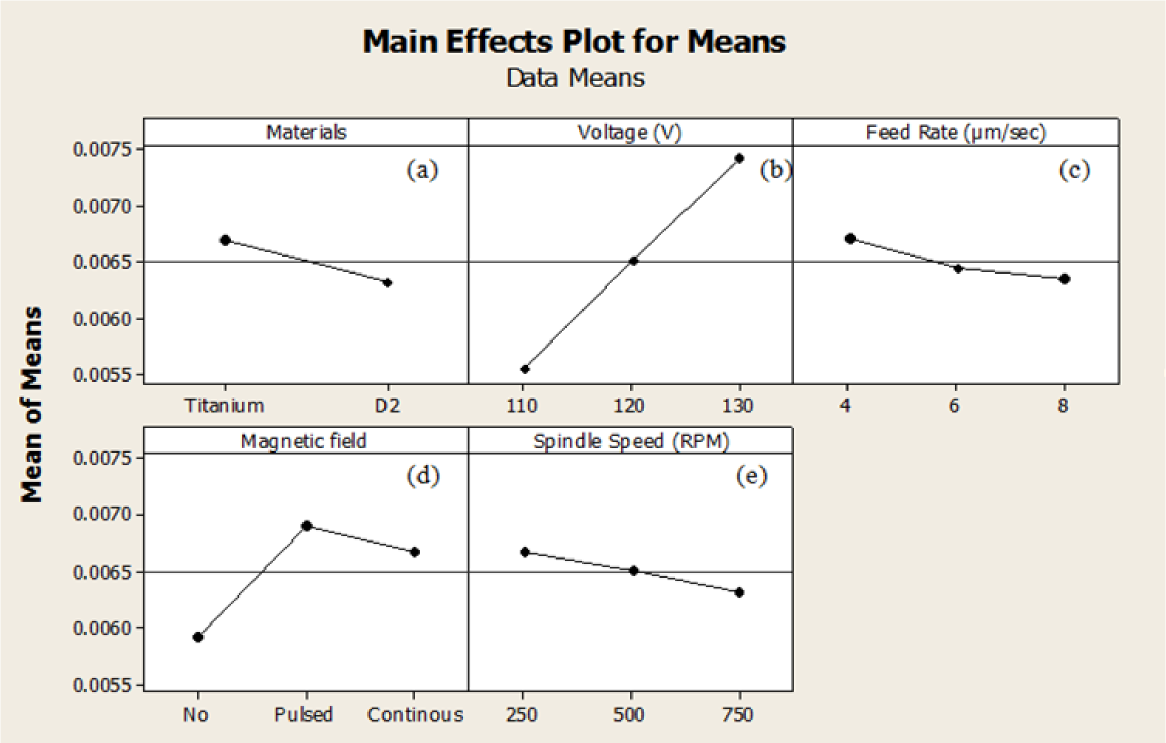

Fig. 3 (a) Effect of type of work-material on MRR (b) Effect of Voltage on MRR
(c) Effect of type of Feed rate on MRR (d) Effect of Electro-magnetic field on MRR
(e) Effect of Spindle Speed on MRR

Fig. 3 (a) shows that the MRR is higher in case of Ti-alloy as compared to D2-steel. This occurs mainly due to the fact that the Ti-alloy has lower value of hardness as compared to D2-steel.

Fig. 3 (b) shows that the increase in MRR is observed at higher value of voltage i.e. at 130V. The general increase in MRR is explained by the fact that the higher the voltage, higher is the energy produced ($E_d = 0.5\ CV^2$) causing to work-material to melt at a faster rate..

Fig. 3 (c) clearly depicts that lower setting of feed rate (4µm/s) gives higher MRR due to the fact that at lower feed rate, short circuit (discharge stop) does not occur so frequently.

The pulsed electro-magnetic field (PEMF) gives higher MRR as shown in fig. 3 (d). This type of behaviour is observed due to fast variation in electro-magnetic field (EMF) strength (upto 0.4T on work-material surface) with each quick change in pulse. This variation in EMF strength leads to high variation in pulling force. This variation in force observed by debris leads to unsettling/non-sticking on either work-material surface as well as on tool. This variation in force is possibly the another reason that more debris comes out from melt pool as compared to when debris feel a continuous equal force during continuous electro-magnetic field setting. These splashed debris now flushes away with di-electric and leads to higher MRR.

Fig. 3 (e) shows that the spindle speed of 250 R.P.M. gives higher value of MRR as compared to 500 R.P.M. and 750 R.P.M. This occurs because Ti-alloy/D2-Steel is considerably tough material to be holed-out and requires proper di-electric ionization during formation of crater on workpiece which is possible when dielectric moves at slow speed.

ANOVA: In subsequent step, ANOVA has been performed to determine the significant factors affecting the output characteristics. The ANOVA for average values of raw data as well as S/N data is given in Tables 7. This Table indicates that all the parameters significantly affect the average values. The percentage contribution of parameters as quantified under column P% in Tables 7 indicates that the voltage, Electro-magnetic field and type of work-materials are the most influential in controlling the average values as well as S/N ratio.

Table 7 ANOVA Of MRR (Means Or Raw Data)

Source	DF	Seq SS	Adj MS (V)	F	SS’	**P %**
Type of Work-materials	1	0.0000019	0.0000019	23.56*	0.0000018	3.696098563
Voltage (V)	2	0.0000314	0.0000157	197.97*	0.0000314	**64.47638604**
Feed Rate (µm/sec)	2	0.0000012	0.0000006	7.59*	0.0000012	2.464065708
Electro-magnetic field	2	0.0000095	0.0000048	59.94*	0.0000095	**19.50718686**
Spindle Speed (R.P.M.)	2	0.0000012	0.0000006	7.63*	0.0000012	2.464065708
Error	44	0.0000035	0.0000001		0.0000035	7.186858316
Total	53	0.0000487			0.0000487	100
*Indicates – Source is Significant at 95% confidence level, SS = Sum of Squares, DOF= Degree of Freedom, SS’= Pure Sum of Squares, F-ratio (1, 44) tabulated for MRR: 4.06, F-ratio tabulated for other parameters: 3.21, P%- Percentage contribution.						

3.1 Estimation of optimum value of MRR

The optimum value of MRR ($mm^3/min.$) is predicted at the selected levels of significant parameters $A_1B_3C_1D_2E_1$. The estimated mean of the response characteristic MRR is determined (Sundaram, Pavalarajan and Rajurkar, 2008; Kumar and Singh, 2014) as

$$\mu_{MRR} = \overline{A}_1 + \overline{B}_3 + \overline{C}_1 + \overline{D}_2 + \overline{E}_1 - 4\times\overline{T} \qquad 2$$

Where T = Overall mean of MRR = 0.006493467, V_e = Error variance = 0.0000001

A_1 (Avg./mean MRR at the first level of Type of Work-material) = 0.00668,

B_3 (Avg./mean MRR at the third level of Voltage) = 0.007417,

C_1 (Avg./mean MRR at the first level of Feed Rate) = 0.006697,

D_2 (Avg./mean MRR at the second level of Electro-magnetic field i.e. Pulsed) = 0.006901,

E_1 (Avg./mean MRR at the first level of Spindle Speed) = 0.00667

Substituting the values of various terms in the above equation

μ_{MRR}=0.00668+0.007417+0.006697+0.006901+0.00667 –4 × 0.006493467 = 0.008391

The 95% confidence interval of confirmation experiments (CI_{CE}) and of population (CI_{pop}) is calculated by using the following equations:

$$CI_{CE} = \sqrt{F_{\alpha}(1,\, f_e)V_e\left[\frac{1}{n_{eff}}+\frac{1}{R}\right]} \tag{3}$$

$$CI_{POP} = \sqrt{\frac{F_{\alpha}(1,\, f_e)V_e}{n_{eff}}} \tag{4}$$

Where $F_{\alpha}(1,f_e)$: The F ratio at the confidence level of (1-α) against DOF 53 and error DOF f_e=44, N: Total number of results = 54 (Treatment=18, Repetition=3), R : Sample size for confirmation experiments =3 V_e: Error variance = 0.0000001(Ref. Anova Table), f_e error DOF = 44. DOF associated in the estimate of mean response = 1+2+2+2+2 = 9

$$n_{eff} = \frac{N}{\text{1+(DOF associated in the estimate of mean response)}} = \frac{54}{1+9} = 5.4 \tag{5}$$

$F_{0.05}(1, 44)$= 4.06 (tabulated F value) , So

$$CI_{CE} = \sqrt{F_{\alpha}(1,\, f_e)V_e\left[\frac{1}{n_{eff}}+\frac{1}{R}\right]} = \sqrt{4.06 * 0.0000001\left[\frac{1}{5.4}+\frac{1}{3}\right]} = \mathbf{0.000458823}$$

$$CI_{POP} = \sqrt{\frac{F_{\alpha}(1,\, f_e)V_e}{n_{eff}}} = \sqrt{\frac{4.06 * 0.0000001}{5.4}} = \mathbf{0.0002742}$$

So CI_{CE}= ±0.000458823, CI_{POP}= ±0.0002742; μ_{MRR}=0.008391

The predicted optimal range (for a confirmation runs of three experiments) is :

$$\mu_{MRR} - CI_{CE} < \mu_{MRR} < \mu_{MRR} + CI_{CE} \text{ is } 0.007932177 < \mu_{MRR} < 0.008849823 \tag{6}$$

The 95% conformation interval of the predicted mean is as follows:

$$\mu_{MRR} - CI_{POP} < \mu_{MRR} < \mu_{MRR} + CI_{POP};\ 0.0081168 < \mu_{MRR} < 0.0086652 \tag{7}$$

3.2 Confirmation experiment

The confirmation test trials to maximize the MRR are conducted at optimal input factors i.e. Type of Work-materials = Ti-alloy (level 1), Voltage (B, level 3) = 130 V, Feed rate (C, level 1) = 4µm/s, Electro-magnetic field (D, level 2) = Pulsed Electro-magnetic Field, Spindle Speed (E, level 1) = 250 R.P.M. The average MRR is found to be 0.008391234 mm^3/min, which fall within the 95% confidence interval of the predicted output factors.

4. CONCLUSIONS:

The present paper investigated the effect of various input parameters on MRR and also the effect of magnetic field in improving the MRR. The significant parameter for MRR is determined by using S/N ratio and ANOVA. The important conclusions are:

(a) The optimal value of process parameters for the predicted range of optimal MRR are as follows: Type of Work-materials (A, level 1), Voltage (B, level 3) = 130 V, Feed rate (C, level 1) = 4µm/s, Electro-magnetic field (D, level 2) = Pulsed Electro-magnetic Field, Spindle Speed (E, level 1) = 250 R.P.M.

(b) MRR increases with increase in voltage, it also seen higher irrespective of magnetic properties of material.

(c) MRR increases when pulsed type EMF is employed. Pulsed EMF provides variable pulling force due to continually change in magnetic strength which results in more molten material removal in discharge column before settling back on surface.

(d) The feed and speed values must be low for hard materials like Titanium alloy and AISI D2-steel.

5. REFERENCES

[1] Alting, L. et al. (2003) ‘Micro engineering’, CIRP Annals - Manufacturing Technology, 52(2), pp. 635–657. doi: 10.1016/S0007-8506(07)60208-X.

[2] Bhattacharya, A., Batish, A. and Bhatt, G. (2015) ‘Material transfer mechanism during magnetic field-assisted electric discharge machining of AISI D2, D3 and H13 die steel’, Proceedings of the Institution of Mechanical Engineers, Part B: Journal of Engineering Manufacture, 229(1), pp. 62–74. doi: 10.1177/0954405414522797.

[3] Chattopadhyay, K. D. et al. (2008) ‘Analysis of rotary electrical discharge machining characteristics in reversal magnetic field for copper-en8 steel system’, International Journal of Advanced Manufacturing Technology, pp. 925–937. doi: 10.1007/s00170-007-1149-y.

[4] Chu, X. et al. (2015) ‘Study on Erosion Mechanism of Magnetic-field-assisted Micro-EDM’, 2(1), pp. 91–95.

[5] Jafferson, J. M., Hariharan, P. and Ram Kumar, J. (2014) 'Effects of ultrasonic vibration and magnetic field in micro-EDM milling of nonmagnetic material', Materials and Manufacturing Processes, 29(3), pp. 357–363. doi: 10.1080/10426914.2013.872268.

[6] Kumar, A. and Satsangi, P. S. (2016) 'Magnetic Field Assisted Micro Edm - a Review', 6913(June).

[7] Kumar, A., Satsangi, P. S., (2014) A Review of Micro Electrical Discharge Machining, Proceedings of National Conference on Advancements and Futuristic Trends in Mechanical Engineering, 60, pp. 346-353.

[8] Kumar, P. and Singh, H. (2014) 'Optimizing Feed Force in Turning Process Using Taguchi's Parameter Design Approach', Applied Mechanics and Materials, 592–594, pp. 668–672. doi: 10.4028/www.scientific.net/AMM.592-594.668.

[9] Kuriakose S. and Shunmugam M.S. (2004), 'Characteristics of Wire Electro Discharge Machined Ti6Al4V Surface', Materials Letters, Vol. 58, pp. 2231-2237.

[10] Prakash, V. et al. (2017) 'Micro-electrical discharge machining of difficult-to-machine materials: A review', Proceedings of the Institution of Mechanical Engineers, Part B: Journal of Engineering Manufacture, 2017, p. 95440541771859. doi: 10.1177/0954405417718591.

[11] Puertas, I., Luis, C. J. and Álvarez, L. (2004) 'Analysis of the influence of EDM parameters on surface quality, MRR and EW of WC-Co', Journal of Materials Processing Technology, 153–154(1–3), pp. 1026–1032. doi: 10.1016/j.jmatprotec.2004.04.346.

[12] S, M. and D, R. (2010) 'Micro-Edm: Overview and Recent Developments', National Conference in Mechanical Engineering Research and Postgraduate Students, 9501(May), pp. 480–494.

[13] Senthilkumar, V. and Omprakash, B. U. (2011) 'Effect of Titanium Carbide particle addition in the aluminium composite on EDM process parameters', Journal of Manufacturing Processes. Elsevier Ltd, 13(1), pp. 60–66. doi: 10.1016/j.jmapro.2010.10.005.

[14] Siva, M., Parivallal, M. and Kumar, M. P. (2014) 'Investigation on the Effect of Process Parameters in Micro Electrical Discharge Machining', Procedia Materials Science, 5, pp. 1829–1836. doi: 10.1016/j.mspro.2014.07.470.

[15] Sundaram, M. M., Pavalarajan, G. B. and Rajurkar, K. P. (2008) 'A study on process parameters of ultrasonic assisted micro EDM based on Taguchi method', Journal of Materials Engineering and Performance, 17(2), pp. 210–215. doi: 10.1007/s11665-007-9128-x.

[16] Takahata, K. and Gianchandani, Y. B. (2002) 'Batch mode micro-electro-discharge machining', Journal of Microelectromechanical Systems, 11(2), pp. 102–110. doi: 10.1109/84.993444.

[17] Wansheng Z., Zhenlong W., Shichun D., Guanxin C. and Hongyu W. (2002), 'Ultrasonic and Electric Discharge Machining to Deep and Small Hole on Titanium Alloy', Journal of Materials Processing Technology, Vol. 120, pp. 101-106.

[18] Yan, B. H. et al. (2002) 'Study of precision micro-holes in borosilicate glass using micro EDM combined with micro ultrasonic vibration machining', International Journal of Machine Tools and Manufacture, 42(10), pp. 1105–1112. doi: 10.1016/S0890-6955(02)00061-5.

[19] Yan M.T. and Lai Y.P. (2007), 'Surface Quality Improvement of Wire EDM Using a Fine-Finish Power Supply', International Journal of Machine Tools and Manufacture, Vol. 47, pp. 1686-1694.

[20] Yu, Z. Y., Masuzawa, T. and Fujino, M. (1998) 'Micro-EDM for Three-Dimensional Cavities - Development of Uniform Wear Method -', CIRP Annals, 47(1), pp. 169–172. doi: 10.1016/S0007-8506(07)62810-8.